

Generalizability through Explainability: Countering Overfitting with Counterfactual Examples

Flavio Giorgi
giorgi@di.uniroma1.it
Sapienza University of Rome
Rome, Italy

Fabrizio Silvestri
fsilvestri@diag.uniroma1.it
Sapienza University of Rome
Rome, Italy

Fabiano Veglianti
fabiano.veglianti@uniroma1.it
Sapienza University of Rome
Rome, Italy

Gabriele Tolomei
tolomei@di.uniroma1.it
Sapienza University of Rome
Rome, Italy

ABSTRACT

Overfitting is a well-known issue in machine learning that occurs when a model struggles to generalize its predictions to new, unseen data beyond the scope of its training set. Traditional techniques to mitigate overfitting include early stopping, data augmentation, and regularization. In this work, we demonstrate that the degree of overfitting of a trained model is correlated with the ability to generate *counterfactual examples*. The higher the overfitting, the easier it will be to find a valid counterfactual example for a randomly chosen input data point. Therefore, we introduce CF-Reg, a novel regularization term in the training loss that controls overfitting by ensuring enough margin between each instance and its corresponding counterfactual. Experiments conducted across multiple datasets and models show that our *counterfactual regularizer* generally outperforms existing regularization techniques.

CCS CONCEPTS

• **Computing methodologies** → **Regularization; Machine learning; Supervised learning.**

KEYWORDS

Overfitting, Generalizability, Regularization, Counterfactual examples, Counterfactual explanations

ACM Reference Format:

Flavio Giorgi, Fabiano Veglianti, Fabrizio Silvestri, and Gabriele Tolomei. YEAR. Generalizability through Explainability: Countering Overfitting with Counterfactual Examples. In *Proceedings of Make sure to enter the correct conference title from your rights confirmation email (Conference acronym 'XX)*. ACM, New York, NY, USA, 9 pages. <https://doi.org/10.1145/nmmnnnn.nmmnnnn>

Permission to make digital or hard copies of all or part of this work for personal or classroom use is granted without fee provided that copies are not made or distributed for profit or commercial advantage and that copies bear this notice and the full citation on the first page. Copyrights for components of this work owned by others than the author(s) must be honored. Abstracting with credit is permitted. To copy otherwise, or republish, to post on servers or to redistribute to lists, requires prior specific permission and/or a fee. Request permissions from permissions@acm.org.
Conference acronym 'XX, MONTH XX–XX, YEAR, LOCATION, XX
© YEAR Copyright held by the owner/author(s). Publication rights licensed to ACM. ACM ISBN 978-1-4503-XXXX-X/18/06...\$15.00
<https://doi.org/10.1145/nmmnnnn.nmmnnnn>

1 INTRODUCTION

One of the key challenges in machine learning is developing models that can generalize their predictions to new, unseen data beyond the scope of the training set. When the predictive accuracy of a model on the training set far exceeds that on the test set, this indicates a phenomenon known as *overfitting*. In general, the impact of overfitting is more pronounced for highly complex models like recent deep neural networks with billions of parameters. To compensate for the risk of overfitting, these models require massive amounts of training data, which may not always be feasible.

Therefore, several strategies have been proposed in the literature to mitigate the problem of model overfitting. For example, *early stopping* interrupts the training phase before the model starts learning the noise in the data rather than the actual underlying input/output relationship. Furthermore, *data augmentation* is a technique that artificially increases the training set. For example, in the context of image data, this can include applying translation, flipping, and rotation transformations to input samples. Finally, *regularization* is a collection of training/optimization techniques that try to eliminate irrelevant factors by assessing the importance of features, preventing minor input changes from causing significant output variations.

In this work, we offer an entirely new perspective on model overfitting, establishing a connection with the ability to generate *counterfactual examples* [28]. The notion of counterfactual examples has been successfully used, for instance, to attach post-hoc explanations for predictions of individual instances in the form: “*If A had been different, B would not have occurred*” [24]. Generally, finding the counterfactual example for an instance resorts to searching for the minimal perturbation of the input that crosses the decision boundary induced by a trained model. This task reduces to solving a constrained optimization problem.

In the presence of a strong degree of model overfitting, the decision boundary learned becomes a highly convoluted surface, up to the point where it perfectly separates every training input sample. Therefore, each data point, on average, is “closer” to the decision boundary, making it easier to find the best counterfactual example. The intuitive explanation of this claim is illustrated in Figure 1.

Following this idea, we introduce a novel *counterfactual regularization* term in the training loss that controls overfitting by enforcing a margin between each instance and its hypothetical

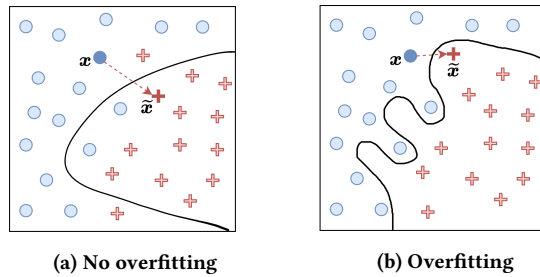


Figure 1: Distance between an input data point (x) and its counterfactual example (\hat{x}): On average, this may be higher for a well-trained model (a) than an overfitted model (b).

counterfactual. Below, we summarize the primary novel contributions of our work:

- (i) We are the first to explore the relationship between generalizability and counterfactual explanations.
- (ii) We show that counterfactual examples can effectively guide and enhance the model training process.
- (iii) We propose a counterfactual regularizer (CF-Reg) that outperforms existing regularization techniques.
- (iv) We cast our regularization method in a flexible and extensible framework that is compatible with any differentiable counterfactual example generator. The source code for our method is available at the following GitHub repository: <https://anonymous.4open.science/r/COCE-80B4/README.md>.

The remainder of this paper is structured as follows. In Section 2, we summarize related work. Section 3 reviews background and preliminary concepts, useful for our problem formulation in Section 4. In Section 5, we describe our method that is validated through extensive experiments in Section 6. We discuss the limitations of our method in Section 7. Finally, Section 8 concludes our work.

2 RELATED WORK

2.1 Model Overfitting

The challenge of model overfitting has been a well-known issue in machine learning. It refers to the inability of a model to generalize effectively from the training dataset to new, unseen test data. Various strategies have been proposed in the literature to reduce the effects of overfitting, which can be broadly categorized as follows.

Early-Stopping. This strategy aims to mitigate the phenomenon known as “learning speed slow-down.” This issue occurs when the accuracy of a model ceases to improve or even worsens due to noise-learning. The concept has a long history, dating back to the 1970s in the context of the Landweber iteration [23]. It has since been widely adopted in iterative algorithms, particularly for training deep neural networks in combination with backpropagation [2].

Data Augmentation. The more complex the model, the higher the number of parameters that need to be learned. Therefore, the size of the training set must be adequate to avoid overfitting. Data augmentation techniques play a crucial role in enhancing model

generalization across various domains, including pattern recognition and image processing. These techniques aim to expand existing datasets to generate additional data. Typically, four main approaches are employed [14, 25, 30]: (i) acquiring new data, (ii) introducing random noise to the existing dataset, (iii) reprocessing existing data to produce new instances, and (iv) sampling new data based on the distribution of the existing dataset.

Regularization. An overfitting model tends to incorporate all available features into its decision-making process, even those with minimal impact or that are simply noise. To address this issue, there are two main approaches: (i) *Feature selection*, where only the most relevant features are retained, discarding those deemed irrelevant; (ii) *Feature regularization*, which involves minimizing the influence of less important features by reducing their weights in the model. However, since identifying useless features can be challenging, regularization techniques work by applying a penalty term, or “regularizer”, to the objective function. This penalizes complex models, encouraging simpler and more generalizable solutions. For example, L_1 (“Lasso”) and L_2 (“Ridge”) regularization, which add the L_1 -norm and L_2 -norm of the learned parameter as a penalties, respectively, are commonly adopted in linear regression. Furthermore, *Dropout* is a popular technique to contrast overfitting in neural networks. This approach randomly drops units and relevant connections from the neural network during training to prevent co-adaptation [29].

Unlike existing regularization techniques, which either aim to reduce the magnitude of the learned model’s weights (such as Lasso and Ridge) or randomly deactivate certain parameters (such as Dropout), our penalty term is inherently *data-driven*. In other words, the counterfactual regularization we introduce (CF-Reg) is computed directly from the training observations, making it highly tailored to the specific dataset under consideration.

Following a similar strategy, Lin et al. (2023) recently proposed a novel regularizer, called *Abnormal Adversarial Examples Regularization* (AAER), which eliminates catastrophic overfitting by suppressing the generation of abnormal adversarial examples.

Although adversarial and counterfactual examples are closely related, AAER addresses a different challenge. Specifically, AAER is designed to mitigate catastrophic overfitting, whereas CF-Reg aims to enhance overall model generalizability.

2.2 Counterfactual Examples

Counterfactual examples have gained significant attention in machine learning due to their utility in various applications, including model *explainability*, *fairness*, and *robustness*.

Explainability. Counterfactual explanations offer valuable insights into model predictions by providing alternative scenarios under which the prediction would change [28]. Several studies have explored the use of counterfactual examples to enhance the interpretability of complex machine learning models, such as ensembles of decision trees [20, 26, 27] and deep neural networks (DNNs) [17], including graph neural networks (GNNs) [21]. Counterfactual instances may elucidate the underlying decision-making process of black-box models, enhancing trust and transparency [3, 7, 13].

Fairness. Counterfactual reasoning has been employed to address issues of fairness and bias in machine learning systems [16]. By generating counterfactual examples, researchers can identify instances

of discrimination or bias in model predictions and mitigate these effects [12]. Various techniques have been proposed to generate counterfactual instances that satisfy fairness constraints, such as demographic parity and equalized odds [28].

Robustness. Counterfactual examples have also been leveraged to enhance the robustness of machine learning models against adversarial attacks [1]. Indeed, there is a strict relationship between adversarial and counterfactual examples [5], although their primary goals are divergent. While both adversarial and counterfactual examples involve perturbing input data to influence model predictions, adversarial examples are crafted to jeopardize the model, whereas counterfactual examples are generated to understand the model’s behavior. By generating instances that are semantically similar to the original input but induce different model predictions, He et al. [9] aim to improve model robustness against adversarial perturbations. These counterfactual examples serve as natural adversaries, enabling the model to learn more robust decision boundaries against malicious attacks.

Recently, generative models have been employed to generate realistic counterfactual instances for data augmentation and model improvement [6, 10]. These approaches offer promising avenues for leveraging counterfactual reasoning in generative modeling tasks [19]. However, to the best of our knowledge, this study is the first to directly link counterfactual examples to model generalizability and leverage them as the cornerstone of a novel regularization method.

3 BACKGROUND AND PRELIMINARIES

Let $f_\theta : \mathcal{X} \mapsto \mathcal{Y}$ denote a predictive model parameterized by a set of (learnable) weights $\theta \in \Theta$ that takes an input $x \in \mathcal{X} \subseteq \mathbb{R}^n$ and maps it to an output $y \in \mathcal{Y}$. In the standard supervised learning setting, the optimal weights (θ^*) are found by minimizing a specific loss function (\mathcal{L}) computed on a training set (\mathcal{D}) of m i.i.d. labeled instances, $\mathcal{D} = \{(x_i, y_i)\}_{i=1}^m$.

$$\theta^* = \arg \min_{\theta} \left\{ \mathcal{L}(\theta; \mathcal{D}) \right\} = \arg \min_{\theta} \left\{ \frac{1}{|\mathcal{D}|} \sum_{i=1}^m \ell(f_\theta(x_i), y_i) \right\}. \quad (1)$$

Here, ℓ represents an instance-level error between the model’s prediction for a given input (x_i) and its corresponding actual label (y_i), such as cross-entropy (for classification tasks) or mean squared error (for regression tasks).

Furthermore, we assume to have available a counterfactual generator model $g_\theta : \mathcal{X} \mapsto \mathcal{X}$, for the predictive model f_θ , that takes as input a data point x and produces as output its corresponding (optimal) counterfactual \tilde{x}^* . We stress that the counterfactual generator model g_θ depends on the predictive model under consideration, since it typically resorts to solving a constrained objective as follows:

$$g_\theta(x) = \tilde{x}^* = \arg \min_{\tilde{x} \in \mathcal{X}} \delta(x, \tilde{x}) \quad \text{s.t.: } f_\theta(x) \neq f_\theta(\tilde{x}). \quad (2)$$

Here, $\delta : \mathcal{X} \times \mathcal{X} \mapsto \mathbb{R}_{\geq 0}$ is a function that measures the distance between the original input data point and its counterfactual. In practice, typically, δ resorts to computing the L_1 - or L_2 -norm of the resulting displacement vector between the original and the counterfactual example.

In general, for a given input x , there could be several, possibly infinitely many *valid* counterfactuals: $\tilde{x}_1, \tilde{x}_2, \dots$. In this work, a valid counterfactual is considered as any instance \tilde{x} where $f_\theta(x) \neq f_\theta(\tilde{x})$. More refined notions of validity are also conceivable, such as those entailing the *plausibility* of the generated counterfactual, which assesses whether the counterfactual example is indeed realistic. For example, suppose we have trained an image classifier to distinguish between birds and rabbits. In this context, a plausible (and valid) counterfactual for a rabbit must be an image showing a bird’s beak. However, for the purpose of this work, we are only interested in characterizing the ability to find a valid counterfactual and relate this to the degree of model overfitting, regardless of its plausibility.

Definition 3.1 (ϵ -Valid Counterfactual Example – ϵ -VCE). Let $x \in \mathcal{X}$ be an input sample, f_θ a trained model, $\delta : \mathcal{X} \times \mathcal{X} \mapsto \mathbb{R}_{\geq 0}$ a distance function, and $\epsilon \in \mathbb{R}_{>0}$ a fixed threshold. Any $\tilde{x} \neq x$, such that $f_\theta(x) \neq f_\theta(\tilde{x})$ and $\delta(x, \tilde{x}) \leq \epsilon$ is an ϵ -valid counterfactual example for x .

4 IMPACT OF COUNTERFACTUAL EXAMPLES ON MODEL GENERALIZABILITY

4.1 Intuition

We consider a training set $\mathcal{D} = \{(x_i, y_i)\}_{i=1}^m$ of m i.i.d. labeled instances, as introduced above. Then, suppose this dataset is used to train a sequence of k different models ($f_{\theta_0}, f_{\theta_1}, \dots, f_{\theta_{k-1}}$). Each model f_{θ_i} is associated with a training accuracy α_i (calculated on \mathcal{D}), such that $\alpha_0 < \alpha_1 < \dots < \alpha_{k-1}$, where f_{θ_0} indicates the random baseline model and $f_{\theta_{k-1}}$ is the dummy model that simply memorizes the entire training set and, therefore, achieves the perfect training accuracy ($\alpha_{k-1} = 1$).

Informally, we claim that for a fixed positive threshold $\epsilon > 0$, the expected number of training points for which we can find an ϵ -valid counterfactual example is positively correlated with the training accuracy of the model. In other words, given two trained models f_{θ_i} and f_{θ_j} , where $i \neq j$, whose training accuracies are $\alpha_i > \alpha_j$, we expect to find, on average, more ϵ -valid counterfactual examples for f_{θ_i} .

This intuition stems from the idea that a model with a higher training accuracy tends to have a more intricate decision boundary surface, which captures all the nuances of the training data more precisely. Consequently, data points are, on average, closer to such a convoluted decision boundary, making it easier for them to find valid counterfactual examples within a distance of ϵ .

In essence, a model for which finding counterfactual examples is “too easy” may indicate a risk of overfitting. Thus, a trade-off must exist between the model’s generalizability and its counterfactual explainability, which we aim to investigate further in this study.

4.2 ϵ -Valid Counterfactual Probability Estimation

To verify our claim, we need to characterize better what we mean by the ease of finding an ϵ -valid counterfactual example for a given data point and, therefore, for a full training set of data points.

Let us consider the generic predictive model f_θ trained on $\mathcal{D} = \{(x_i, y_i)\}_{i=1}^m$. Suppose we associate to each training data point x_i a binary random variable $X_i \in \{0, 1\}$, which indicates whether there

exists an ε -valid counterfactual example \tilde{x}_i for x_i . Therefore, each X_i follows a Bernoulli distribution, i.e., $X_i \sim \text{Bernoulli}(p_i^\varepsilon)$, whose probability mass function is defined as below.

$$\mathbb{P}(X_i = k) = p_{X_i}(k; p_i^\varepsilon) = \begin{cases} p_i^\varepsilon & , \text{if } k = 1 \\ 1 - p_i^\varepsilon & , \text{if } k = 0. \end{cases} \quad (3)$$

Furthermore, let \bar{X} define the average number of training points for which we can find an ε -valid counterfactual example. More formally, $\bar{X} = \frac{1}{m} \sum_{i=1}^m X_i$ is the average of m Bernoulli random variables. Thus, we can calculate $\mathbb{E}[\bar{X}] = \mathbb{E}\left[\frac{1}{m} \sum_{i=1}^m X_i\right] = \frac{1}{m} \sum_{i=1}^m \mathbb{E}[X_i]$ due to the linearity of expectation, where $\mathbb{E}[X_i] = p_i^\varepsilon$. Note that the random variable $Z = \sum_{i=1}^m X_i$ follows a Poisson-Binomial distribution since X_i 's are independent but not necessarily identically distributed. Overall, $\bar{X} = \frac{Z}{m}$, which scales the Poisson-Binomial random variable Z by $1/m$, namely $\bar{X} \sim \text{Poisson-Binomial}(\lambda)$, where $\lambda = \frac{1}{m} \sum_{i=1}^m p_i^\varepsilon$.

For a fixed $\varepsilon > 0$, we claim $\mathbb{E}[\bar{X}]$ to be positively correlated with the training accuracy of the model. Simply put, as the training accuracy of f_θ increases, we foresee a corresponding increase in the expected average number of training data points for which a valid counterfactual example can be found within a distance of ε .

Ultimately, the task aims to estimate each p_i^ε , which we call the (sample-level) ε -valid counterfactual probability.

Definition 4.1 (ε -Valid Counterfactual Probability – ε -VCP). Let f_θ be a trained model, $x \in X \subseteq \mathbb{R}^n$ a generic training point, and $\varepsilon \in \mathbb{R}_{>0}$ a positive real number. Consider the ε -ball as the n -dimensional hypersphere of radius ε centered around x . Let $V_x^\varepsilon \subseteq \mathbb{R}^n$ be the total hypervolume of such hypersphere and let $V_x^\varepsilon \subseteq V_x^\varepsilon$ denote the portion of the total hypervolume falling within the counterfactual region delimited by the decision boundary induced by f_θ . Therefore, we can estimate the ε -valid counterfactual probability (ε -VCP) for x , as $p^\varepsilon = V_x^\varepsilon / V_x^\varepsilon$.

It is worth noticing that, in practice, x can be seen as an embedding from an autoencoding process, mapping each raw training point into a dense, lower-dimensional latent manifold within the original, high-dimensional space.

Thus, our focus is to evaluate how easily a counterfactual generation method can identify a counterfactual example within ε , given an input sample x . Intuitively, given a fixed x and two different models having different decision boundaries, it will generally be much easier to find an ε -valid counterfactual if the hypervolume V_x^ε is larger. This intuition is depicted in Figure 2, which illustrates how the probability of finding an ε -valid counterfactual for a 2-dimensional data point may increase with model overfitting.

To estimate V_x^ε , we can apply standard Monte Carlo integration, a well-established technique that uses random draws to numerically compute a definite integral. Furthermore, using Monte Carlo integration will provide valuable knowledge on the shape of a model's decision boundary as a by-product. The estimate outlined above assumes that data points are uniformly distributed around x in the latent space, which may be reasonable for appropriate values of ε . More accurate estimates could be obtained by sampling the ε -neighborhood from the manifold using advanced strategies (e.g., see Chen et al. [3]). However, this lies beyond the primary scope of this step and will be explored in future work.

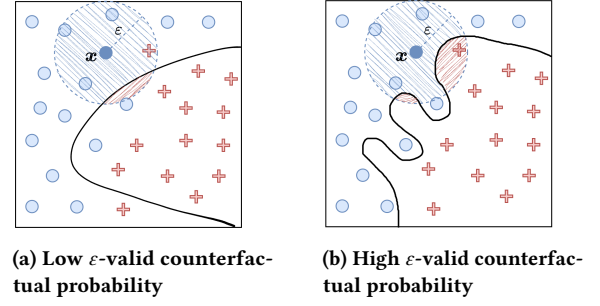


Figure 2: The ε -valid counterfactual probability for a sample $x \in \mathbb{R}^2$ can be estimated as the ratio of the area of the circle centered in x with radius ε that falls behind the decision boundary (in red).

Finally, if we extend the same reasoning above to all training points, we should observe that the expected average number of training points for which we find ε -valid counterfactual examples ($\mathbb{E}[\bar{X}]$) should be higher for overtrained models.

4.3 Empirical Assessment

To investigate the impact of overfitting on ε -VCP, we trained two Multi-Layer Perceptron (MLP) models on the *Water Potability* dataset [11] for a binary classification task. Both models used the same 5-layer architecture, but only one applied dropout regularization with a dropout rate of 0.5. The models were trained over 500 epochs using the Adam optimizer with a learning rate of $\eta = 0.001$. Finally, the ε -VCP was estimated through Monte Carlo integration as discussed in Section 4.2. Specifically, we calculated it as $p^\varepsilon = V_x^\varepsilon / V_x^\varepsilon$, where $\varepsilon = 1.5$ and V_x^ε was estimated using 100 random samples for each training point x .

It is important to note that the choice of ε depends on the underlying dataset. A good practice is to empirically determine this value to ensure a meaningful assessment of counterfactual validity while maintaining consistency with the dataset structure. Specifically, since ε represents the maximum norm of the perturbation vector applied to each sample, it serves as a threshold that defines the allowable search space for counterfactuals. A value that is too small would overly restrict counterfactual perturbations, limiting the ability to assess meaningful changes in predictions. Conversely, a value that is too large could result in unrealistic perturbations that deviate from the underlying data distribution. In this experiment with the *Water Potability* dataset, we found that setting $\varepsilon = 1.5$ provides a suitable trade-off, allowing us to capture a diverse yet interpretable range of counterfactual examples without introducing excessive modifications to the original training points.

Figure 3 illustrates the evolution of the average ε -VCP, calculated over all training points, as a function of the models' training accuracy. From this plot, three key insights emerge. First, the average ε -VCP increases alongside training accuracy for both models, confirming our hypothesis that the likelihood of finding valid counterfactuals rises as models tend to overfit. Second, the plain, unregularized MLP exhibits higher ε -VCP values, suggesting that its more complex decision boundary makes it easier to identify

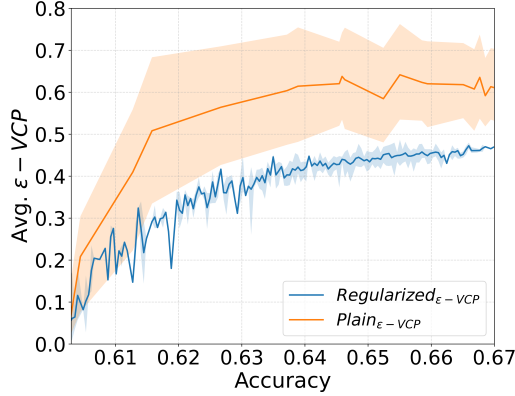


Figure 3: The average ε -VCP (y-axis) as a function of the model’s training accuracy (x-axis). $Plain_{\varepsilon-VCP}$ is the “vanilla” MLP, while $Regularized_{\varepsilon-VCP}$ is the same MLP yet with a dropout rate of 0.5.

valid counterfactual examples. Third, the trend persists while the MLP trained with dropout regularization exhibits a less pronounced increase (i.e., smaller ε -VCP values). This suggests that although dropout regularization smooths the decision boundary to some extent, it may not sufficiently counteract this phenomenon, leaving room for further improvement.

5 COUNTERFACTUAL REGULARIZATION

5.1 A New Training Loss

We exploit the correlation between overfitting and the ability to find counterfactual examples, as highlighted in the previous section, to define a new regularized training loss as follows.

$$\theta^* = \arg \min_{\theta} \left\{ \mathcal{L}_{\text{emp}}(\theta; \mathcal{D}) - \alpha \mathcal{L}_{\text{cf}}(\theta; \mathcal{D}, \varepsilon) \right\}. \quad (4)$$

The first term (\mathcal{L}_{emp}) is the standard empirical risk, while the second term (\mathcal{L}_{cf}) is our proposed *counterfactual regularization* component, with $\alpha \in \mathbb{R}_{\geq 0}$ serving as a hyperparameter to weigh its contribution. More specifically, the counterfactual regularization component can be defined as follows:

$$\mathcal{L}_{\text{cf}}(\theta; \mathcal{D}, \varepsilon) = \varphi(\{d(x_i, g_{\theta}(x_i)), x_i \in \mathcal{D}\}; \varepsilon), \quad (5)$$

where $\varphi(\cdot; \varepsilon)$ – parameterized by ε – acts as an aggregation function applied to the set of distances $d(x_i, g_{\theta}(x_i))$ between each sample x_i and its corresponding counterfactual generated by the model, $g_{\theta}(x_i)$. Intuitively, the closer an instance is to its counterfactual, the greater the penalty imposed by the newly introduced loss. In other words, optimizing the objective defined in (4) aims to ensure a sufficient margin between each training point and its corresponding counterfactual. Moreover, we would like this penalty to be stronger for training points where finding a counterfactual is easier – i.e., those closer to the decision boundary. To achieve this goal, each distance $d(x_i, g_{\theta}(x_i))$ can be assigned a weight w_i^{ε} that depends on ε during aggregation. For example, this weight may be set as the ε -valid counterfactual probability associated with each training instance x_i (i.e., $w_i^{\varepsilon} = p_i^{\varepsilon}$).

Note that, for each data point x_i , its corresponding p_i^{ε} can be estimated as described in Section 4.2. However, since p_i^{ε} depends on the shape of the decision boundary, which may evolve dynamically across training epochs, its estimation should ideally be updated at *every* epoch. However, this could introduce a significant computational overhead in the training process, which we can mitigate by instead updating our estimates $\{p_i^{\varepsilon}\}_{i=1}^m$ periodically, for example, every t epochs. We conjecture that a trade-off exists between the effectiveness of the counterfactual regularization term – impacted by the accuracy of each estimate p_i^{ε} – and the computational cost of the training process.

It is worth noting that our counterfactual regularizer – hereinafter referred to as CF-Reg – is flexible enough to support any choice of aggregation function (φ), distance (d), and counterfactual generator (g_{θ}). However, the optimization problem in (4) can be efficiently solved using standard gradient-based methods, provided that φ , d , and g_{θ} are all differentiable with respect to θ .

In this work, we set φ as the mean, d as the Euclidean distance (i.e., the L_2 -norm of the displacement vector resulting from the difference between the original sample and its corresponding counterfactual). For g_{θ} , we adopt the *score counterfactual explanation* method proposed by Wachter et al. [28], and we discuss the rationale behind this choice below. Alternative formulations of these components are possible and will be explored in future studies.

5.2 Counterfactual Example Generator

A key component of CF-Reg is the counterfactual generator g_{θ} , as this is used to compute the optimal counterfactual example for each training data point. To incorporate this step into the regularized training process, the counterfactual generator must satisfy two essential requirements. First, it must be differentiable with respect to the predictive model weights θ . Second, it must be highly efficient to ensure the overall feasibility of our method. Among the various counterfactual generation approaches in the literature, we have selected the score counterfactual explanation method proposed by [28], which is defined as follows.

Definition 5.1 (Score Counterfactual Explanation). Let $x \in \mathcal{X}$ be an input sample, f_{θ} a trained model, $\delta : \mathcal{X} \times \mathcal{X} \mapsto \mathbb{R}_{\geq 0}$ a distance function, $\beta \in \mathbb{R}_{\geq 0}$ a controlling hyperparameter, and $s \in \mathbb{R}$ a target score. Thus, the score counterfactual explanation \tilde{x} for x is the result of the following optimization problem:

$$\tilde{x}^* = \arg \min_{\tilde{x} \in \mathcal{X}} (f_{\theta}(\tilde{x}) - s)^2 + \beta \delta(x, \tilde{x}). \quad (6)$$

With a slight abuse of notation, in (6), we treat the output of the predictive model f_{θ} as a continuous value, even for classification tasks. To accommodate this requirement, we can, for instance, assume access to the logits, which are then passed through the appropriate activation function, such as sigmoid or softmax.

Note that the resulting counterfactual generator satisfies the two requirements mentioned above. In particular, by carefully selecting the distance function δ in (6), the resulting objective becomes differentiable with respect to the predictive model weights θ . Furthermore, when using the score-based counterfactual explanation approach, determining the optimal counterfactual perturbation vector $\delta = x - \tilde{x}^* = x - g_{\theta}(x)$ – i.e., the displacement vector between the original instance and its optimal counterfactual – admits a

closed-form solution under specific assumptions. Specifically, if f_θ is a linear function and $\tilde{\mathbf{x}}^* = g_\theta(\mathbf{x})$ is the optimal counterfactual example for the input \mathbf{x} , Pawelczyk et al. [22] proved that:

$$\delta = \frac{t}{\beta + \|\theta\|^2} \cdot \theta, \quad (7)$$

where $t = s - f_\theta(\mathbf{x})$. This makes the method highly efficient and well-suited for incorporation into our regularized training loss.

From (7), we can, therefore, compute the L_2 -norm of the perturbation vector δ_i , for each training instance x_i . This value is then used as $d(x_i, \tilde{x}_i^*)$, as required by the proposed regularized training loss in (5). Finally, the L_2 -norms of all perturbation vectors are aggregated using the function $\varphi(\cdot; \varepsilon)$, resulting in the following (weighted) average:

$$\overline{\|\delta\|} = \frac{1}{m} \sum_{i=1}^m w_i^\varepsilon * \|\delta_i\|. \quad (8)$$

In the simplest case, the weights are uniformly set as $w_i^\varepsilon = 1 \forall i \in \{1, \dots, m\}$, effectively reducing the aggregation to a standard average. Alternatively, more sophisticated strategies can be employed, such as the approach outlined in Section 5.1, where each training point is assigned a weight corresponding to its estimated ε -VCP, i.e., $w_i^\varepsilon = p_i^\varepsilon$.

Overall, this transforms our counterfactual regularized loss as follows:

$$\theta^* = \arg \min_{\theta} \left\{ \mathcal{L}_{\text{emp}}(\theta; \mathcal{D}) - \alpha \overline{\|\delta\|} \right\}. \quad (9)$$

Finally, the objective in (9) can be solved using standard gradient-based optimization methods.

6 EXPERIMENTS

The experiments are designed to address two key research questions. First, **RQ1** evaluates whether the average L_2 -norm of the counterfactual perturbation vectors ($\overline{\|\delta\|}$) decreases as the model overfits the data, thereby providing further empirical validation for our hypothesis. Second, **RQ2** evaluates the ability of the proposed counterfactual regularized loss, as defined in (9), to mitigate overfitting when compared to existing regularization techniques.

6.1 Experimental Setup

Datasets, Models, and Tasks. The experiments are conducted on three datasets: *Water Potability* [11], *Phomene* [4], and *CIFAR-10* [15]. For *Water Potability* and *Phomene*, we randomly select 80% of the samples for the training set, and the remaining 20% for the test set, *CIFAR-10* comes already split. Furthermore, we consider the following models: Logistic Regression, Multi-Layer Perceptron (MLP) with 100 and 30 neurons on each hidden layer, and PreactResNet-18 [8] as a Convolutional Neural Network (CNN) architecture. We focus on binary classification tasks and leave the extension to multiclass scenarios for future work. However, for datasets that are inherently multiclass, we transform the problem into a binary classification task by selecting two classes, aligning with our assumption.

Evaluation Measures. To characterize the degree of overfitting, we use the test loss, as it serves as a reliable indicator of the model’s generalization capability to unseen data. Additionally, we evaluate the predictive performance of each model using the test accuracy.

Baselines. We compare CF-Reg with the following regularization techniques: L1 (“Lasso”), L2 (“Ridge”), and Dropout.

Configurations. For each model, we adopt specific configurations as follows.

- **Logistic Regression:** To induce overfitting in the model, we artificially increase the dimensionality of the data beyond the number of training samples by applying a polynomial feature expansion. This approach ensures that the model has enough capacity to overfit the training data, allowing us to analyze the impact of our counterfactual regularizer. The degree of the polynomial is chosen as the smallest degree that makes the number of features greater than the number of data.
- **Neural Networks (MLP and CNN):** To take advantage of the closed-form solution for computing the optimal perturbation vector as defined in (7), we use a local linear approximation of the neural network models. Hence, given an instance x_i , we consider the (optimal) counterfactual not with respect to f_θ but with respect to:

$$f_\theta^{\text{lin}}(\mathbf{x}) = f_\theta(\mathbf{x}_i) + \nabla_{\mathbf{x}} f_\theta(\mathbf{x}_i)(\mathbf{x} - \mathbf{x}_i), \quad (10)$$

where f_θ^{lin} represents the first-order Taylor approximation of f_θ at \mathbf{x}_i . Note that this step is unnecessary for Logistic Regression, as it is inherently a linear model.

Implementation Details. We run all experiments on a machine equipped with an AMD Ryzen 9 7900 12-Core Processor and an NVIDIA GeForce RTX 4090 GPU. Our implementation is based on the PyTorch Lightning framework. We use stochastic gradient descent as the optimizer with a learning rate of $\eta = 0.001$ and no weight decay. We use a batch size of 128. The training and test steps are conducted for 6000 epochs on the *Water Potability* and *Phoneme* datasets, while for the *CIFAR-10* dataset, they are performed for 200 epochs. Finally, the contribution w_i^ε of each training point x_i is uniformly set as $w_i^\varepsilon = 1 \forall i \in \{1, \dots, m\}$.

The source code implementation for our experiments is available at the following GitHub repository: <https://anonymous.4open.science/r/COCE-80B4/README.md>

6.2 RQ1: Counterfactual Perturbation vs. Overfitting

To address **RQ1**, we analyze the relationship between the test loss and the average L_2 -norm of the counterfactual perturbation vectors ($\overline{\|\delta\|}$) over training epochs.

In particular, Figure 4 depicts the evolution of $\overline{\|\delta\|}$ alongside the test loss for an MLP trained *without* regularization on the *Water Potability* dataset.

The plot shows a clear trend as the model starts to overfit the data (evidenced by an increase in test loss). Notably, $\overline{\|\delta\|}$ begins to decrease, which aligns with the hypothesis that the average distance to the optimal counterfactual example gets smaller as the model’s decision boundary becomes increasingly adherent to the training data.

It is worth noting that this trend is heavily influenced by the choice of the counterfactual generator model. In particular, the relationship between $\overline{\|\delta\|}$ and the degree of overfitting may become

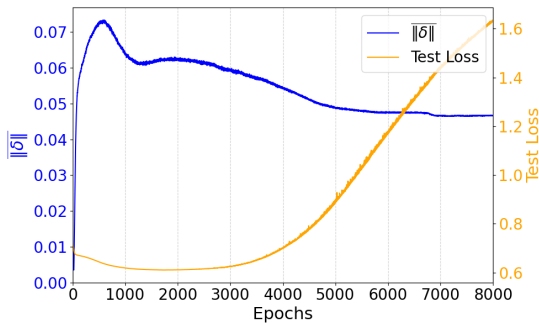


Figure 4: The average counterfactual perturbation vector $\|\delta\|$ (left y -axis) and the cross-entropy test loss (right y -axis) over training epochs (x -axis) for an MLP trained on the *Water Potability* dataset without regularization.

even more pronounced when leveraging more accurate counterfactual generators. However, these models often come at the cost of higher computational complexity, and their exploration is left to future work.

Nonetheless, we expect that $\|\delta\|$ will eventually stabilize at a plateau, as the average L_2 -norm of the optimal counterfactual perturbations cannot vanish to zero.

6.3 RQ2: Counterfactual Regularization Performance

To answer RQ2, we evaluate the effectiveness of the proposed counterfactual regularization (CF-Reg) by comparing its performance against existing baselines: unregularized training loss (No-Reg), L1 regularization (L1-Reg), L2 regularization (L2-Reg), and Dropout. Specifically, for each model and dataset combination, Table 1 presents the mean value and standard deviation of test accuracy achieved by each method across 5 random initialization.

The table illustrates that our regularization technique consistently delivers better results than existing methods across all evaluated scenarios, except for one case – i.e., Logistic Regression on the *Phomene* dataset. However, this setting exhibits an unusual pattern, as the highest model accuracy is achieved without any regularization. Even in this case, CF-Reg still surpasses other regularization baselines.

From the results above, we derive the following key insights. First, CF-Reg proves to be effective across various model types, ranging from simple linear models (Logistic Regression) to deep architectures like MLPs and CNNs, and across diverse datasets, including both tabular and image data. Second, CF-Reg’s strong performance on the *Water* dataset with Logistic Regression suggests that its benefits may be more pronounced when applied to simpler models. However, the unexpected outcome on the *Phoneme* dataset calls for further investigation into this phenomenon.

6.4 Feasibility of our Method

A crucial requirement for any regularization technique is that it should impose minimal impact on the overall training process. In this respect, CF-Reg introduces an overhead that depends on the

time required to find the optimal counterfactual example for each training instance. As such, the more sophisticated the counterfactual generator model probed during training the higher would be the time required. However, a more advanced counterfactual generator might provide a more effective regularization. We discuss this trade-off in more details in Section 7.

Table 3 presents the average training time (\pm standard deviation) for each model and dataset combination listed in Table 1. We can observe that the higher accuracy achieved by CF-Reg using the score-based counterfactual generator comes with only minimal overhead. However, when applied to deep neural networks with many hidden layers, such as *PreactResNet-18*, the forward derivative computation required for the linearization of the network introduces a more noticeable computational cost, explaining the longer training times in the table.

6.5 Hyperparameter Sensitivity Analysis

The proposed counterfactual regularization technique relies on two key hyperparameters: α and β . The former is intrinsic to the loss formulation defined in (2), while the latter is closely tied to the choice of the score-based counterfactual explanation method used.

Figure 5 illustrates how the test accuracy of an MLP trained on the *Water Potability* dataset changes for different combinations of α and β .

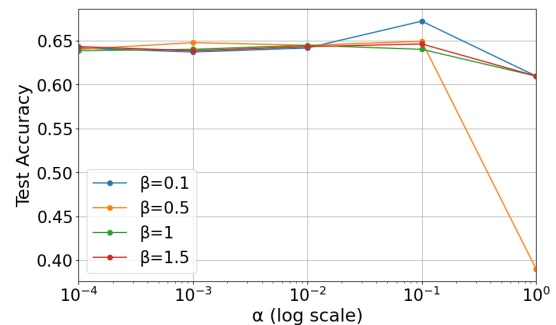


Figure 5: The test accuracy of an MLP trained on the *Water Potability* dataset, evaluated while varying the weight of our counterfactual regularizer (α) for different values of β .

We observe that, for a fixed β , increasing the weight of our counterfactual regularizer (α) can slightly improve test accuracy until a sudden drop is noticed for $\alpha > 0.1$. This behavior was expected, as the impact of our penalty, like any regularization term, can be disruptive if not properly controlled.

Moreover, this finding further demonstrates that our regularization method, CF-Reg, is inherently data-driven. Therefore, it requires specific fine-tuning based on the combination of the model and dataset at hand.

7 CURRENT LIMITATIONS

In this section, we discuss the current limitations of CF-Reg and identify potential areas for improvement. It is important to note that, in this initial iteration, our primary goal was to minimize the impact of our method on the overall training process. As a

Table 1: Mean value and standard deviation of test accuracy across 5 random initializations for different model, dataset, and regularization method. The best results are highlighted in bold.

Model	Dataset	No-Reg	L1-Reg	L2-Reg	Dropout	CF-Reg (ours)
Logistic Regression	<i>Water</i>	0.6595 ± 0.0038	0.6729 ± 0.0056	0.6756 ± 0.0046	N/A	0.6918 ± 0.0036
MLP	<i>Water</i>	0.6756 ± 0.0042	0.6790 ± 0.0058	0.6790 ± 0.0023	0.6750 ± 0.0036	0.6802 ± 0.0046
Logistic Regression	<i>Phomene</i>	0.8148 ± 0.0020	0.8041 ± 0.0028	0.7835 ± 0.0176	N/A	0.8098 ± 0.0055
MLP	<i>Phomene</i>	0.8677 ± 0.0033	0.8374 ± 0.0080	0.8673 ± 0.0045	0.8672 ± 0.0042	0.8718 ± 0.0040
CNN	<i>CIFAR-10</i>	0.6670 ± 0.0233	0.6229 ± 0.0850	0.7348 ± 0.0365	N/A	0.7427 ± 0.0571

Table 2: Hyperparameter configurations utilized for the generation of Table 1. For our regularization the hyperparameters are reported as α/β .

Model	Dataset	No-Reg	L1-Reg	L2-Reg	Dropout	CF-Reg (ours)
Logistic Regression	<i>Water</i>	N/A	0.0093	0.6927	N/A	0.3791/1.0355
MLP	<i>Water</i>	N/A	0.0007	0.0022	0.0002	0.2567/1.9775
Logistic Regression	<i>Phomene</i>	N/A	0.0097	0.7979	N/A	0.0571/1.8516
MLP	<i>Phomene</i>	N/A	0.0007	$4.24 \cdot 10^{-5}$	0.0015	0.0516/2.2700
CNN	<i>CIFAR-10</i>	N/A	0.0050	0.0864	N/A	0.3018/2.1502

Table 3: Mean value and standard deviation of training time across 5 different runs. The reported time (in seconds) corresponds to the generation of each entry in Table 1. Times are

Model	Dataset	No-Reg	L1-Reg	L2-Reg	Dropout	CF-Reg (ours)
Logistic Regression	<i>Water</i>	222.98 ± 1.07	239.94 ± 2.59	241.60 ± 1.88	N/A	251.50 ± 1.93
MLP	<i>Water</i>	225.71 ± 3.85	250.13 ± 4.44	255.78 ± 2.38	237.83 ± 3.45	266.48 ± 3.46
Logistic Regression	<i>Phomene</i>	266.39 ± 0.82	367.52 ± 6.85	361.69 ± 4.04	N/A	310.48 ± 0.76
MLP	<i>Phomene</i>	335.62 ± 1.77	390.86 ± 2.11	393.96 ± 1.95	363.51 ± 5.07	403.14 ± 1.92
CNN	<i>CIFAR-10</i>	370.09 ± 0.18	395.71 ± 0.55	401.38 ± 0.16	N/A	1287.8 ± 0.26

result, we prioritized efficiency, which may have come at the cost of potentially higher accuracy.

First, the framework proposed in Section 5.1 is designed to accommodate *any* counterfactual generator g_θ . However, this flexibility may come at the cost of increased computational overhead, as each training point requires querying g_θ to generate the corresponding counterfactual example. The feasibility of the training process thus depends on the efficiency of g_θ . For instance, when using a relatively simple generator, such as the score-based counterfactual model adopted in this work, the impact on overall training time is minimal, as shown in the previous section, though this may come at the expense of regularization performance. Conversely, employing a more sophisticated g_θ could improve generalization but at the cost of significantly increased training time. This highlights an inherent trade-off between the complexity of the counterfactual generation process and the effectiveness of the regularization it provides. The exploration of more complex counterfactual generators is, therefore, a promising direction for future research.

Second, even when using the score-based counterfactual generator, we might not fully exploit the closed-form solution for calculating the optimal perturbation vector as shown in (7). This analytical solution is valid under the assumption that the predictive model f_θ is a linear function of the input parameters. However, when f_θ is a deep neural network, this assumption is typically violated, and we approximate it using the first-order Taylor expansion, as

in (10). This approximation, while useful, could lead to suboptimal counterfactuals, as it may not fully capture the non-linearity of the model’s behavior.

Third, the results presented are based on a straightforward weighting scheme for CF-Reg, where the contribution w_i^e of each training point \mathbf{x}_i is uniformly set as $w_i^e = 1 \forall i \in \{1, \dots, m\}$. A more fine-grained strategy could potentially enhance the quality of the regularization, although it would likely increase the training time.

8 CONCLUSION AND FUTURE WORK

We introduced and analyzed the trade-off between the generalizability and explainability of predictive models, highlighting their often conflicting nature. Specifically, we demonstrated that the degree of model overfitting is positively correlated with its ability to generate counterfactual examples. Building on this insight, we proposed CF-Reg, a novel regularization technique that integrates a counterfactual regularization term into the training objective, to balance between predictive performance and interpretability.

Through extensive experiments across multiple datasets and model architectures, we showed that CF-Reg generally outperforms existing regularization techniques, improving generalization while maintaining the ability to generate meaningful counterfactual explanations. Our results suggest that counterfactual-based regularization can serve as a principled approach to improving model robustness without sacrificing interpretability.

However, we acknowledge that there is significant room for improvement, and we outline several promising directions for future research. First, we plan to explore more sophisticated counterfactual generation methods, which could enhance the effectiveness of our regularization strategy by generating more informative perturbations. Second, we aim to investigate adaptive weighting strategies that dynamically adjust the regularization strength for each training instance based on its proximity to the decision boundary.

REFERENCES

- [1] Tom B Brown, Nicholas Carlini, Chiyuan Zhang, Catherine Olsson, Paul Christiano, and Ian Goodfellow. 2018. Unrestricted Adversarial Examples. *arXiv preprint arXiv:1809.08352* (2018).
- [2] Rich Caruana, Steve Lawrence, and C. Giles. 2000. Overfitting in Neural Nets: Backpropagation, Conjugate Gradient, and Early Stopping. In *Advances in Neural Information Processing Systems*, T. Leen, T. Dietterich, and V. Tresp (Eds.), Vol. 13. MIT Press, 381–387. https://proceedings.neurips.cc/paper_files/paper/2000/file/059fdcd96baeb75112f09fa1dcc740cc-Paper.pdf
- [3] Ziheng Chen, Fabrizio Silvestri, Jia Wang, He Zhu, Hongshik Ahn, and Gabriele Tolomei. 2022. ReLAX: Reinforcement Learning Agent Explainer for Arbitrary Predictive Models. In *Proceedings of the 31st ACM International Conference on Information & Knowledge Management (Atlanta, GA, USA) (CIKM '22)*. Association for Computing Machinery, New York, NY, USA, 252–261. <https://doi.org/10.1145/3511808.3557429>
- [4] Thomson-Sintra Dominique Van Cappel. 1993. Phoneme. https://www.openml.org/search?type=data&sort=version&status=any&order=asc&exact_name=phoneme&id=1489.
- [5] Timo Freiesleben. 2022. The Intriguing Relation Between Counterfactual Explanations and Adversarial Examples. *Minds and Machines* 32, 1 (mar 2022), 77–109. <https://doi.org/10.1007/s11023-021-09580-9>
- [6] Yaroslav Ganin, Evgeniya Ustinova, Hana Ajakan, Pascal Germain, Hugo Larochelle, François Laviolette, Mario Marchand, and Victor Lempitsky. 2016. Domain-Adversarial Training of Neural Networks. *Journal of Machine Learning Research* 17, 1 (jan 2016), 2096–2030.
- [7] Riccardo Guidotti, Anna Monreale, Salvatore Ruggieri, Dino Pedreschi, Franco Turini, and Fosca Giannotti. 2018. Local Rule-Based Explanations of Black Box Decision Systems. *arXiv preprint arXiv:1805.10820* (2018).
- [8] Kaiming He, Xiangyu Zhang, Shaoqing Ren, and Jian Sun. 2016. Identity Mappings in Deep Residual Networks. In *Computer Vision – ECCV 2016*, Bastian Leibe, Jiri Matas, Nicu Sebe, and Max Welling (Eds.). Springer International Publishing, Cham, 630–645.
- [9] Zecheng He, Tianwei Zhang, and Ruby B. Lee. 2019. Model inversion attacks against collaborative inference. In *Proceedings of the 35th Annual Computer Security Applications Conference (San Juan, Puerto Rico, USA) (ACSAC '19)*. Association for Computing Machinery, New York, NY, USA, 148–162. <https://doi.org/10.1145/3359789.3359824>
- [10] R. Devon Hjelm, Alex Fedorov, Samuel Lavoie-Marchildon, Karan Grewal, Philip Bachman, Adam Trischler, and Yoshua Bengio. 2019. Learning Deep Representations by Mutual Information Estimation and Maximization. In *7th International Conference on Learning Representations, ICLR 2019, New Orleans, LA, USA, May 6–9, 2019*. OpenReview.net. <https://openreview.net/forum?id=Bklr3j0cKX>
- [11] Aditya Kadiwal. 2020. Water Potability Dataset. <https://www.kaggle.com/datasets/adityakadiwal/water-potability> Accessed: 2025-01-27.
- [12] Faisal Kamiran and Toon Calders. 2012. Data Preprocessing Techniques for Classification without Discrimination. *Knowledge and Information Systems* 33, 1 (2012), 1–33.
- [13] Amir-Hossein Karimi, Gilles Barthe, Borja Balle, and Isabel Valera. 2020. Model-Agnostic Counterfactual Explanations for Consequential Decisions. In *International Conference on Artificial Intelligence and Statistics*. PMLR, 895–905.
- [14] G.N. Karystinos and D.A. Pados. 2000. On Overfitting, Generalization, and Randomly Expanded Training Sets. *IEEE Transactions on Neural Networks* 11, 5 (2000), 1050–1057. <https://doi.org/10.1109/72.870038>
- [15] Alex Krizhevsky. 2009. Learning Multiple Layers of Features from Tiny Images. (2009), 32–33. <https://www.cs.toronto.edu/~kriz/learning-features-2009-TR.pdf>
- [16] Matt Kusner, Joshua Loftus, Chris Russell, and Ricardo Silva. 2017. Counterfactual Fairness. In *Proceedings of the 31st International Conference on Neural Information Processing Systems (Long Beach, California, USA) (NeurIPS '17)*. Curran Associates Inc., Red Hook, NY, USA, 4069–4079.
- [17] Thai Le, Suhang Wang, and Dongwon Lee. 2020. GRACE: Generating Concise and Informative Contrastive Sample to Explain Neural Network Model's Prediction (KDD '20). Association for Computing Machinery, New York, NY, USA, 238–248. <https://doi.org/10.1145/3394486.3403066>
- [18] Runqi Lin, Chaojian Yu, and Tongliang Liu. 2023. Eliminating Catastrophic Overfitting via Abnormal Adversarial Examples Regularization. In *Proceedings of the 37th International Conference on Neural Information Processing Systems (New Orleans, LA, USA) (NeurIPS '23)*. Curran Associates Inc., Red Hook, NY, USA, Article 2968, 20 pages.
- [19] Romain Lopez, Adam Gayoso, and Nir Yosef. 2020. Enhancing Scientific Discoveries in Molecular Biology with Deep Generative Models. *Molecular Systems Biology* 16, 9 (2020), e9198. <https://doi.org/10.15252/msb.20199198> arXiv:<https://www.embopress.org/doi/pdf/10.15252/msb.20199198>
- [20] Ana Lucic, Harrie Oosterhuis, Hinda Haned, and Maarten de Rijke. 2022. FOCUS: Flexible Optimizable Counterfactual Explanations for Tree Ensembles. In *Proceedings of the AAAI conference on artificial intelligence*, Vol. 36. 5313–5322.
- [21] Ana Lucic, Maartje A. Ter Hoeve, Gabriele Tolomei, Maarten De Rijke, and Fabrizio Silvestri. 2022. CF-GNNExplainer: Counterfactual Explanations for Graph Neural Networks. In *Proceedings of The 25th International Conference on Artificial Intelligence and Statistics (Proceedings of Machine Learning Research, Vol. 151)*, Gustau Camps-Valls, Francisco J. R. Ruiz, and Isabel Valera (Eds.). PMLR, 4499–4511. <https://proceedings.mlr.press/v151/lucic22a.html>
- [22] Martin Pawelczyk, Chirag Agarwal, Shalmali Joshi, Sohini Upadhyay, and Himabindu Lakkaraju. 2022. Exploring Counterfactual Explanations Through the Lens of Adversarial Examples: A Theoretical and Empirical Analysis. In *Proceedings of The 25th International Conference on Artificial Intelligence and Statistics (Proceedings of Machine Learning Research, Vol. 151)*, Gustau Camps-Valls, Francisco J. R. Ruiz, and Isabel Valera (Eds.). PMLR, 4574–4594. <https://proceedings.mlr.press/v151/pawelczyk22a.html>
- [23] Garvesh Raskutti, Martin J. Wainwright, and Bin Yu. 2011. Early Stopping for Non-Parametric Regression: An Optimal Data-Dependent Stopping Rule. In *2011 49th Annual Allerton Conference on Communication, Control, and Computing (Allerton)*, 1318–1325. <https://doi.org/10.1109/Allerton.2011.6120320>
- [24] Ilia Stepin, Jose M Alonso, Alejandro Catala, and Martín Pereira-Fariña. 2021. A Survey of Contrastive and Counterfactual Explanation Generation Methods for Explainable Artificial Intelligence. *IEEE Access* 9 (2021), 11974–12001.
- [25] Yi Sun, Xiaogang Wang, and Xiaoou Tang. 2014. Deep Learning Face Representation from Predicting 10,000 Classes. In *2014 IEEE Conference on Computer Vision and Pattern Recognition*. 1891–1898. <https://doi.org/10.1109/CVPR.2014.244>
- [26] Gabriele Tolomei and Fabrizio Silvestri. 2021. Generating Actionable Interpretations from Ensembles of Decision Trees. *IEEE Transactions on Knowledge and Data Engineering* 33, 4 (2021), 1540–1553. <https://doi.org/10.1109/TKDE.2019.2945326>
- [27] Gabriele Tolomei, Fabrizio Silvestri, Andrew Haines, and Mounia Lalmas. 2017. Interpretable Predictions of Tree-based Ensembles via Actionable Feature Tweaking (KDD '17). Association for Computing Machinery, New York, NY, USA, 465–474. <https://doi.org/10.1145/3097983.3098039>
- [28] Sandra Wachter, Brent Mittelstadt, and Chris Russell. 2017. Counterfactual Explanations without Opening the Black Box: Automated Decisions and the GDPR. *Harvard Journal of Law & Technology*, 31 (2017), 841–887.
- [29] David Warde-Farley, Ian J. Goodfellow, Aaron C. Courville, and Yoshua Bengio. 2014. An Empirical Analysis of Dropout in Piecewise Linear Networks. In *2nd International Conference on Learning Representations, ICLR 2014, Banff, AB, Canada, April 14–16, 2014, Conference Track Proceedings*, Yoshua Bengio and Yann LeCun (Eds.). <http://arxiv.org/abs/1312.6197>
- [30] Kevin Y. Yip and Mark Gerstein. 2008. Training Set Expansion: An Approach to Improving the Reconstruction of Biological Networks from Limited and Uneven Reliable Interactions. *Bioinformatics* 25, 2 (11 2008), 243–250. <https://doi.org/10.1093/bioinformatics/btn602> arXiv:https://academic.oup.com/bioinformatics/article-pdf/25/2/243/48983145/bioinformatics_25_2_243.pdf